Spectroscopic properties of $Nd_{0.5}Gd_{0.5}Fe_3(BO_3)_4$ single crystal

A.V. Malakhovskii*, A.L. Sukhachev, A.A. Leont'ev, I.A. Gudim, A.S. Krylov, A.S. Aleksandrovsky

L.V. Kirensky Institute of Physics, Siberian Branch, Russian Academy of Sciences, 660036 Krasnoyarsk, Russian Federation

ARTICLE INFO

ABSTRACT

The polarized absorption spectra of trigonal single crystal $Nd_{0.5}Gd_{0.5}Fe_3(BO_3)_4$ were measured in the spectral range 10,000–22,000 cm^{-1}. The *d–d* and *f–f* transitions spectra were separated. The *f–f* transitions intensities were analyzed in terms of the Judd–Ofelt theory in a ferroborate with huntite structure for the first time, and the following parameters of the theory were obtained: $\Omega_2 = 4.4 \times 10^{-20}$ cm^2, $\Omega_4 = 8.04 \times 10^{-20}$ cm^2, and $\Omega_6 = 8.25 \times 10^{-20}$ cm^2. The strengths, spontaneous emission probabilities, branching ratios, spectroscopic quality factor and excited state lifetime were calculated for transitions from the $^4F_{3/2}$ state to ^4I_J manifold. All the obtained spectroscopic characteristics were compared with those of alumoborates with the same crystal structure.

1. Introduction

The spectroscopic properties of neodymium ions in various crystalline matrices remain the subject of continuous interest of researchers (see, e.g., recent publications [1–4] and references therein). Special interest is connected with Nd^{3+} ions in borate matrices with huntite structure. Borates $RM_3(BO_3)_4$ (R–Y or rare earth (RE) metal, M–Al, Ga, Cr, Fe, Sc) are trigonal crystals with huntite-like structure (space group $R32$ (D_3^7)) without center of inversion. Therefore, crystals of this type can be used as self-doubling laser media. In particular, optical, luminescent, nonlinear and laser properties of neodymium containing alumoborates were studied in a number of works (e.g., [5–12]). To the best of our knowledge, there were no similar works concerning ferroborates. Optical spectra and crystal field parameters of $NdFe_3(BO_3)_4$ were studied in Ref. [13]. Nearest relatives of the crystal under study, $NdFe_3(BO_3)_4$ and $GdFe_3(BO_3)_4$, the same as some other RE ferroborates, refer to multiferroics [14–18], which simultaneously possess magnetic and electric order. Therefore, it is possible to suppose that our crystal is also multiferroic. The first measurements [19] confirm this assumption. All RE ferroborates are magnetically ordered at temperatures below 30–40 K. In particular, $Nd_{0.5}Gd_{0.5}Fe_3(BO_3)_4$ crystal becomes antiferromagnetic at $T = 32$ K [20]. The changes of

magnetic and electric states of the RE ferroborates, both caused by the phase transitions or by the external fields, substantially influence the parameters of the *f–f* absorption spectra [21–26]. Such possibility exists also due to the optical magneto-electric effects [27–30].

In this paper we present measurements of polarized absorption spectra of the $Nd_{0.5}Gd_{0.5}Fe_3(BO_3)_4$ single crystal. The parity forbidden *f–f* transitions spectra are treated with the help of the Judd–Ofelt theory, and spectroscopic parameters obtained are compared with those of some other compounds, in particular, with those of alumoborates of the same crystal structure.

2. Experimental details

$Nd_{0.5}Gd_{0.5}Fe_3(BO_3)_4$ single crystals were grown from the melt solution on the base of $K_2Mo_3O_{10}$ as described in Ref. [31]. At room temperature, the crystal belongs to trigonal symmetry class with the space group $R32$, the lattice constants of the grown crystals being: $a = 9.557(7)$ Å and $c = 7.62(1)$ Å [20]. The unit cell (Fig. 1) contains three formula units. Trivalent rare-earth (RE) ions occupy positions of only one type. They are located at the center of trigonal prisms made up of six crystallographically equivalent oxygen ions. The triangles formed by the oxygen ions in the neighboring basal planes are not superimposed on each other but are twisted by a certain angle. Owing to this distortion, the symmetry D_{3h} of the ideal prism is reduced to the symmetry D_3 [32]. The FeO_6 octahedrons share edges in such a way that they form helicoidal chains, which run parallel to the C_3 axis and are mutually independent. At room temperature all Fe ions occupy C_2-symmetry positions in the crystal.

The absorption spectra were measured with the light propagating normally to the C_3 axis of the crystal for the light electric vector $\vec{E}$ parallel (π spectrum) and perpendicular (σ spectrum) to the C_3 axis, and for the light propagating along the C_3 axis (α spectrum). The spectral resolution was approximately equal to 10 cm^{-1}.

* Corresponding author. Tel.: +7 391 2498617; fax: +7 391 2438923.
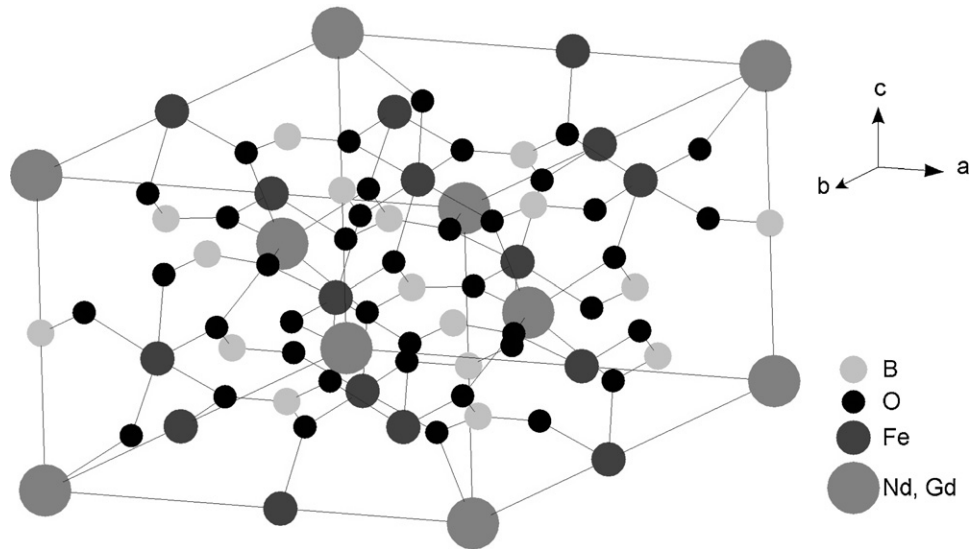*E-mail address:* malakha@iph.krasn.ru (A.V. Malakhovskii).

Fig. 1. Crystal lattice of the $Nd_{0.5}Gd_{0.5}Fe_3(BO_3)_4$ single crystal.

Absorption spectra of the $Nd_{0.5}Gd_{0.5}Fe_3(BO_3)_4$ crystal for π and σ polarizations at room temperature are shown in Fig. 2 (decimal absorption coefficients). The absorption spectra measured in the σ and α polarizations coincide within the limit of the experimental error. This implies that the absorption mainly occurs through the electric dipole mechanism.

3. Results and discussion

Absorption spectra of $Nd_{0.5}Gd_{0.5}Fe_3(BO_3)_4$ crystal (Fig. 2) consist both of narrow bands corresponding to f–f transitions in Nd^{3+} ions and of wide bands due to d–d transitions in Fe^{3+} ions ($^6A_1 \rightarrow {}^4T_1$ and $^6A_1 \rightarrow {}^4T_2$ in cubic crystal field notation). At $E \sim 22{,}900\,cm^{-1}$ comparatively strong d–d transition $^6A_1 \rightarrow {}^4A_1\,{}^4E$ is observed, and at $E \sim 25{,}000\,cm^{-1}$ the edge of the strong absorption occurs, which is due to interatomic Fe–Fe transitions and to charge transfer transitions $2p \rightarrow 3d$ between molecular 2p-orbitals of ligands and 3d-orbitals of the Fe^{3+} ion inside FeO_6 cluster.

During the analysis of spectra, first of all, we erased the f–f absorption bands from the total spectra. The remained spectra we approximated by the Gauss functions, and thereby d–d spectra were obtained separately (Fig. 2). Then we subtracted the d–d spectra from the total spectra and obtained the f–f spectra

(Figs. 3–5 demonstrate f–f spectra at room temperature and at $T = 90\,K$). Identification of the f–f spectra was made according to Ref. [33] and labels are assigned according to Ref. [34]. Separated f–f and d–d spectra permitted to find integral intensities of the absorption bands (Tables 1 and 2). Transition intensities were averaged over the polarizations according common relation for uniaxial anisotropic crystals: $I = (2I_\sigma + I_\pi)/3$. Following the Ref. [35], we calculated oscillator strengths of transitions $I \rightarrow F$ between J multiplets by the formula:

$$f_{IF} = 4.318 \times 10^{-9} \frac{3n}{(n)^2 + 2} I_{IF} \qquad (1)$$

Here the integral intensity is given in units of $cm^{-2}\,mol^{-1}\,l$. The refractive index measured in the reflected light was found to be $n = 1.44 \pm 0.02$. The determined oscillator strengths of f–f and d–d transitions are given in Tables 1 and 2. The transition strength is defined as: $s_{IF} = 1/e^2 \sum_{if} |\vec{D}_{if}|^2$, where $i \in I$, $f \in F$. The transition
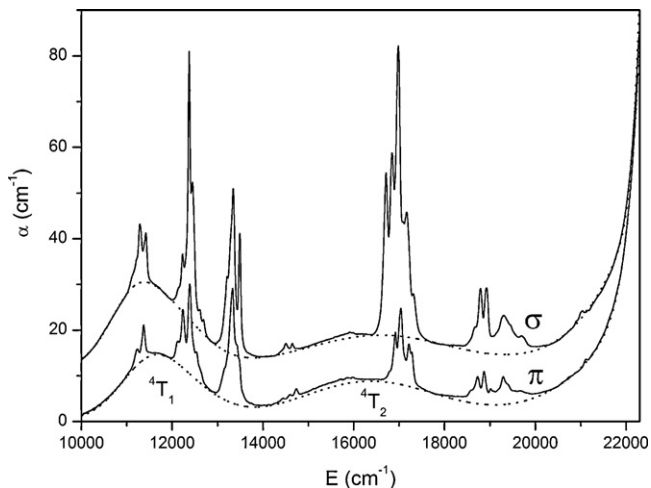
Fig. 2. π- and σ-polarized absorption spectra of the $Nd_{0.5}Gd_{0.5}Fe_3(BO_3)_4$ single crystal at room temperature.
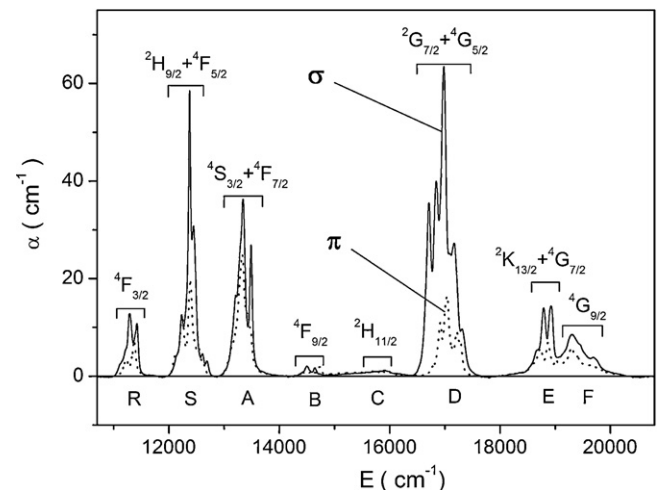
Fig. 3. π- and σ-polarized absorption spectra of f–f transitions in the $Nd_{0.5}Gd_{0.5}Fe_3(BO_3)_4$ single crystal at room temperature.

Table 1
Parameters of f–f transitions in Nd^{3+} ion in the $Nd_{0.5}Gd_{0.5}Fe_3(BO_3)_4$ single crystal at room temperature: average wave numbers k_{IF}, integrated intensities I_{IF}, oscillator strengths f_{IF}, transition strengths s_{IF}.

Symbol	Transition $^4I_{9/2}\downarrow$	k_{IF} (cm^{-1})	I_{IF} (cm^{-2} mol^{-1} l)			f_{IF} (10^{-7})	s_{IF} (10^{-20} cm^2)	
			σ	π	$(2\sigma+\pi)/3$		Measured	Calculated
R	$^4F_{3/2}$	11,360	650	270	520	24.0	1.95	2.3
S	$^2H_{9/2}+{}^4F_{5/2}$	12,350	2100	1080	1760	80.6	6.01	6.27
A	$^4S_{3/2}+{}^4F_{7/2}$	13,330	2080	1420	1860	85.2	5.9	5. 8
B	$^4F_{9/2}$	14,600	130	90	120	5.5	0.35	0.4
C	$^2H_{11/2}$	15,800	130	150	140	6.4	0.37	0.11
D	$^2G_{7/2}+{}^4G_{5/2}$	16,970	5220	1100	3850	176	9.56	9.61
E + F	$^4G_{7/2}+{}^4G_{9/2}+{}^2K_{13/2}$	19,000	2040	1150	1740	79.7	3.87	3.09

Table 2
Parameters of d–d transitions in Fe^{3+} ion in the $Nd_{0.5}Gd_{0.5}Fe_3(BO_3)_4$ single crystal at room temperature: wave numbers k_{IF}, integrated intensities I_{IF} and oscillator strengths f_{IF}.

Transition $^6A_1\downarrow$	k_{IF} (cm^{-1})	I_{IF} (cm^{-2} mol^{-1} l)			f_{IF} (10^{-7})
		σ	π	$(2\sigma+\pi)/3$	
$^4T_1$	11,360	1440	1150	1340	58
$^4T_2$	12,350	1100	1280	1160	50
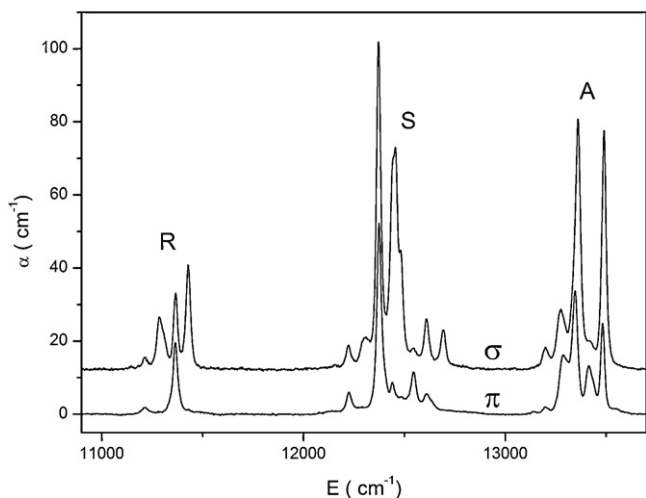
Fig. 4. Fragment of π- and σ-polarized absorption spectra of f–f transitions in the $Nd_{0.5}Gd_{0.5}Fe_3(BO_3)_4$ single crystal at 90 K.
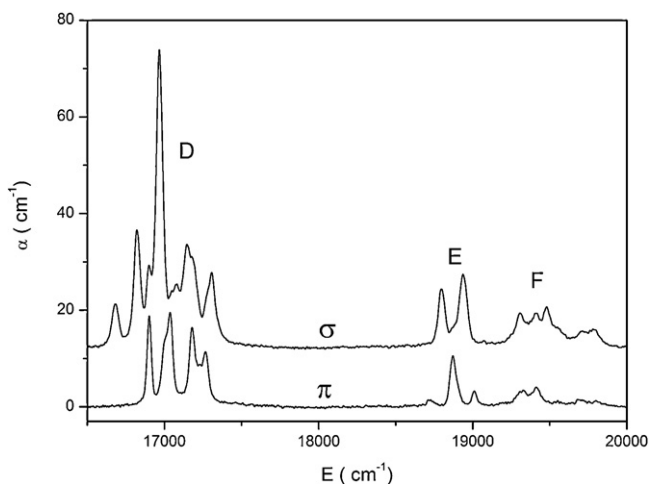
Fig. 5. Fragment of π- and σ-polarized absorption spectra of f–f transitions in the $Nd_{0.5}Gd_{0.5}Fe_3(BO_3)_4$ single crystal at 90 K.

strength and the oscillator strength are related by the expression [36]

$$s_{IF}=\frac{3hg_I}{8\pi^2 mck_{IF}}f_{IF} \qquad (2)$$

where g_I is the degree of degeneracy of the initial state and k_{IF} is the average wave number of the absorption band. Experimentally found strengths of the f–f transitions are given in Table 1. Comparison of strengths of the transitions in $Nd_{0.5}Gd_{0.5}Fe_3(BO_3)_4$ with those in some alumoborates is presented in Table 3. In spite of the identical symmetry of the crystals, intensities of the transitions are substantially different: the smallest intensities, close to each other, are in crystals with the doping level of order of several per cent, and the largest ones are in the stoichiometric neodymium alumoborate. The crystal under study, $Nd_{0.5}Gd_{0.5}Fe_3(BO_3)_4$ stands in the intermediate position. Thus, the largest non-centrosymmetrical distortions are in the stoichiometric neodymium alumoborate.

Both d–d and f–f transitions are parity-forbidden ones. Some of the observed f–f transitions are also formally spin-forbidden ones. However, the spin–orbit interaction in $4f$ states is so strong that only the total moment is the good quantum number, and the spin-forbiddenness is practically removed. All d–d transitions in Fe^{3+} ($3d^5$) ion are strongly spin-forbidden since the spin–orbit interaction is small and the crystal field is large. Nevertheless, intensities of d–d and f–f transitions observed in the $Nd_{0.5}Gd_{0.5}Fe_3(BO_3)_4$ crystal are of the same order of magnitude (see Tables 1 and 2). There are two reasons of this fact. A strong exchange interaction between Fe^{3+} ions (T_N = 32 K) give rise to effective exchange mechanism of removal of the spin-forbiddenness [37]. The covalency of metal–ligand bonding plays very important role in the allowance by parity [38], and this parameter is much larger for $3d$ ions than for $4f$ ions.

In the framework of the Judd–Ofelt theory, the strength of an f–f transition in an ion in the non-centrosymmetrical crystal field is described by the relationship [39–41]

$$s_{IF}=\sum_\lambda \Omega_\lambda \Gamma_\lambda^2(I,F) \qquad (3)$$

Coefficients $\Gamma_\lambda^2(I,F)=\langle I\|U^{(\lambda)}\|F\rangle^2$ are calculated theoretically [33] and are considered to be independent of crystal structure. The index λ for the f–f transitions takes three values: 2, 4, and 6. Therefore, it is sufficient to find experimentally the strengths of any three transitions in order to determine three parameters Ω_λ and to

Table 3
Measured strengths (10^{-20} cm^2) of f–f transitions in crystals: Nd$_{0.5}$Gd$_{0.5}$Fe$_3$(BO$_3$)$_4$ (NGFB), NdAl$_3$(BO$_3$)$_4$ (NAB), Nd:GdAl$_3$(BO$_3$)$_4$ (NGAB) and Nd:Gd$_{0.2}$Y$_{0.8}$Al$_3$(BO$_3$)$_4$ (NGYAB).

Symbol	Transition $^4I_{9/2} \downarrow$	NGFB [this work]	NAB [10]	NGAB [10]	NGYAB [10]
R	$^4F_{3/2}$	1.95	3.27	0.99	0.85
S	$^2H_{9/2} + {}^4F_{5/2}$	6.01	10.53	3.22	3.46
A	$^4S_{3/2} + {}^4F_{7/2}$	5.9	9.35	3.24	3.43
B	$^4F_{9/2}$	0.35	0.91	–	0.19
C	$^2H_{11/2}$	0.37	0.38	–	–
D	$^2G_{7/2} + {}^4G_{5/2}$	9.56	12.30	5.64	4.56
E + F	$^4G_{7/2} + {}^4G_{9/2} + {}^2K_{13/2}$	3.87	4.45	1.69	1.85

calculate the strengths of all the other transitions. The transitions under consideration in a free Nd^{3+} ion are forbidden in the electric dipole approximation not only by the parity, but some of them are forbidden by the total momentum in accordance with the selection rule $\Delta J = 0, \pm 1$. According to the Judd–Ofelt theory [41], when transitions are allowed by the parity selection rule due to the odd components of the crystal field, they can occur at $\Delta J \le \lambda$ ($\lambda = 2, 4,$ and 6 as mentioned above). Therefore, within this approximation, all considered f–f transitions in the Nd^{3+} ion are allowed.

Eq. (3) can be written in the vector form:

$$s = A\Omega \qquad (4)$$

Here s is a q-dimensional vector consisting of the measured strengths of the transition groups; q is the number of the considered groups of transitions; Ω is the three-dimensional vector of parameters Ω_λ; A is the $3 \times q$-dimensional matrix of coefficients $\Gamma_\lambda^2(I, F)$. The vector Ω that minimizes the sum of the squares of the deviations between the measured and theoretical transition strengths is given by the matrix equation [42]

$$\Omega = (A^T A)^{-1} A^T s, \qquad (5)$$

where A^T is the transposed matrix. We used five most intense groups of the transitions: $R, S, A, D, (E+F)$, and obtained parameters Ω_λ shown in Table 4. Judd–Ofelt parameters of some neodymium containing alumoborates and those of other crystals are also given in Table 4. We see again that properties of f–f transitions are very sensitive to the local environment of the $4f$ ions. Even nominally identical crystals NdAl$_3$(BO$_3$)$_4$ have substantially different parameters Ω_λ (Table 4). The relative root mean square error of the theoretical description of the transition strengths is defined by equation

$$\delta = \left[\frac{q \sum \Delta s^2}{(q-p) \sum s^2} \right]^{1/2} \qquad (6)$$

Here s are the measured transition strengths, Δs are the differences between the measured and calculated transition strengths, p is the number of the determined parameters, being equal to 3 in our case. With the help of (6) and Table 1 we obtain $\delta \approx 11\%$.

One of the main postulates of the Judd–Ofelt theory is the equal population of all crystal field splitted components of the ground state. The splitting of the ground state of Nd^{3+} ion in the crystals of huntite structure is approximately equal to 320 cm^{-1} (460 K) [9,13]. Therefore, the mentioned postulate is not satisfied at room temperature, and the transition intensities can change with the temperature. Indeed, the intensity of one of the absorption bands substantially changes with the temperature (Fig. 6). This implies that the intensity at room temperature, taken for the calculations, is not correct, and application of the Judd–Ofelt theory becomes nonrigorous, that results in a discrepancy between the experiment and theory. For example, it is known that there are substantial difficulties in description of praseodymium spectra by the Judd–Ofelt theory [45]. Indeed, intensities of Pr^{3+} transitions in glasses strongly depend on temperature [46]. Apart from the basic assumptions underlying the Judd–Ofelt theory,

there are also other reasons that reduce the accuracy of its application. The wave numbers k_{IF} in the expression (2) are rather approximate and uncertain quantities for broad absorption bands, and they differ for absorption and emission because the adiabatic potentials are different for different electronic states. It is also important that the equilibrium configuration of atoms can be different in different electronic states and, therefore, the crystal field modifying the electron wave functions can also be different. This is most significant for the electronic transitions forbidden by the parity, because they become allowed as a result of small odd distortions of the crystal field. Furthermore, the system in the excited state can relax to a new equilibrium configuration during the long lifetime. As a result, the matrix elements of the electric dipole moment can depend on the transition direction (upward or downward). Therefore, the change in the atomic configuration during the electronic transition can be one of the reasons that some transitions do not obey the Judd–Ofelt theory.

Now, when we know Ω_λ parameters, we can find with the help of Eq. (3) the strengths of transitions not observed in the absorption spectra, in particular, the strengths of the laser transitions from the $^4F_{3/2}$ state (Table 5). Coefficients Γ_λ^2 were taken from Ref. [47]. Probability of a spontaneous dipole transition between degenerate levels in a condensed matter is given by the relationship [48]

$$A_{IF} = \frac{64\pi^4 e^2 k_{IF}^3 n(k_{IF})}{3 h g_I} s_{IF} \qquad (7)$$

Here g_I is the degeneracy of the initial multiplet, and $n(k_{IF})$ is the refractive index at the transition frequency (as we noted above, it is taken equal to 1.44). In order to find values of k_{IF} for transitions between excited states, we used positions of ^4I states given in Ref. [13] for NdFe$_3$(BO$_3$)$_4$. The possibility of generating of stimulated
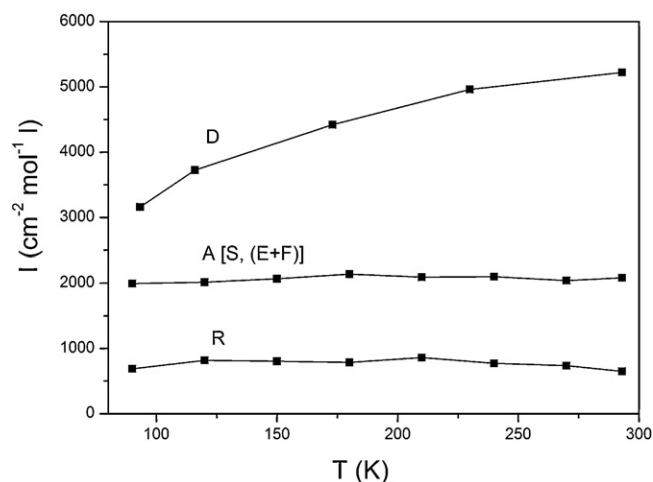

Fig. 6. Temperature dependences of the f–f absorption bands integral intensities in α-polarization. The intensities of A, S and $(E+F)$ bands are practically identical.

[8] D. Jaque, O. Enguita, J. García Solé, A.D. Jiang, Z.D. Luo, Appl. Phys. Lett. 76 (2000) 2176.
[9] D. Jaque, O. Enguita, U.G. Caldiño, M.O. Ramírez, J. García Solé, J. Appl. Phys. 90 (2001) 561.
[10] X. Chen, Z. Luo, D. Jaque, J.J. Romero, J. García Solé, J. Phys.: Condens. Matter. 13 (2001) 1171.
[11] M. Huang, Y. Chen, X. Chen, Y. Huang, Z. Luo, Opt. Commun. 208 (2002) 163.
[12] A. Majchrowski, S. Klosowicz, L.R. Jaroszewicz, M. Swirkowicz, I.V. Kityk, M. Piasecki, M.G. Brik, J. Alloy Compd. 491 (2010) 26.
[13] M.N. Popova, E.P. Chukalina, T.N. Stanislavchuk, B.Z. Malkin, A.R. Zakirov, E. Antic-Fidancev, E.A. Popova, L.N. Bezmaternykh, V.L. Temerov, Phys. Rev. B 75 (2007) 224435.
[14] A.K. Zvezdin, S.S. Krotov, A.M. Kadomtseva, G.P. Vorob'ev, Y.F. Popov, A.P. Pyatakov, L.N. Bezmaternykh, E.A. Popova, Pis'ma v ZhETF 81 (2005) 335 (JETP Lett. 81 (2005) 272).
[15] A.K. Zvezdin, G.P. Vorob'ev, A.M. Kadomtseva, Yu.F. Popov, A.P. Pyatakov, L.N. Bezmaternykh, A.V. Kuvardin, E.A. Popova, Pis'ma v ZhETF 83 (2006) 600 (JETP Lett. 83 (2006) 509).
[16] F. Yen, B. Lorenz, Y.Y. Sun, C.W. Chu, L.N. Bezmaternykh, A.N. Vasiliev, Phys. Rev. B 73 (2006) 054435.
[17] A.M. Kadomtseva, Yu.F. Popov, G.P. Vorob'ev, A.A. Muhin, V.Yu. Ivanov, A.M. Kuzmenko, L.N. Bezmaternykh, Pis'ma v ZhETF 87 (2008) 45 (JETP Lett. 87 (2008) 39).
[18] R.P. Chaudhury, F. Yen, B. Lorenz, Y.Y. Sun, L.N. Bezmaternykh, V.L. Temerov, C.W. Chu, Phys. Rev. B 80 (2009) 104424.
[19] A.M. Kadomtseva, Yu.F. Popov, G.P. Vorob'ev, A.A. Mukhin, V.Yu. Ivanov, A.M. Kuz'menko, A.S. Prokhorov, L.N. Bezmaternykh, V.L. Temerov, I.A. Gudim, Proceedings of the XXI International Conference New in Magnetism and Magnetic Materials, Moscow, 2009, p. 316.
[20] A.V. Malakhovskii, E.V. Eremin, D.A. Velikanov, A.V. Kartashev, A.D. Vasil'ev, I.A. Gudim, Fiz. Tverd. Tela 53 (2011) 1929 (Phys. Solid State 53 (2011) 2032).
[21] M.N. Popova, E.P. Chukalina, T.N. Stanislavchuk, L.N. Bezmaternykh, JMMM 300 (2006) e440.
[22] T.N. Stanislavchuk, E.P. Chukalina, M.N. Popova, L.N. Bezmaternykh, I.A. Gudim, Phys. Lett. A 368 (2007) 408.
[23] Ph. Goldner, O. Guillot-Noël, J. Petit, M. Popova, L. Bezmaternykh, Phys. Rev. B 76 (2007) 165102.
[24] M.N. Popova, T.N. Stanislavchuk, B.Z. Malkin, L.N. Bezmaternykh, Phys. Rev. B 80 (2009) 195101.
[25] E.P. Chukalina, M.N. Popova, L.N. Bezmaternykh, I.A. Gudim, Phys. Lett. A 374 (2010) 1790.
[26] A.V. Malakhovskii, S.L. Gnatchenko, I.S. Kachur, V.G. Piryatinskaya, A.L. Sukhachev, V.L. Temerov, Eur. Phys. J. B 80 (2011) 1.
[27] B.B. Krichevtsov, V.V. Pavlov, R.V. Pisarev, V.N. Gridnev, Phys. Rev. Lett. 76 (1996) 4628.
[28] J.H. Jung, M. Matsubara, T. Arima, J.P. He, Y. Kaneko, Y. Tokura, Phys. Rev. Lett. 93 (2004) 037403.
[29] Y. Shimada, H. Kiyama, Y. Tokura, Phys. Rev. B 75 (2007) 245125.
[30] T. Arima, J. Phys.: Condens. Matter 20 (2008) 434211.
[31] A.D. Balaev, L.N. Bezmaternykh, I.A. Gudim, V.L. Temerov, S.G. Ovchinnikov, S.A. Kharlamova, J. Magn. Magn. Mater. 258–259 (2003) 532.
[32] I. Couwenberg, K. Binnemans, H. De Leebeeck, C. Görller-Walrand, J. Alloy Compd. 274 (1998) 157.
[33] W.T. Carnall, P.R. Fields, B.G. Wybourne, J. Chem. Phys. 42 (1965) 3797.
[34] G.H. Dieke, Spectra and Energy Levels of Rare Earth Ions in Crystals, Interscience Publishers, New York/London/Sydney/Toronto, 1968.
[35] A.V. Malakhovskii, A.E. Sokolov, V.L. Temerov, L.N. Bezmaternykh, A.L. Sukhachev, V.A. Seredkin, S.L. Gnatchenko, I.S. Kachur, V.G. Piryatinskaya, Fiz. Tverd. Tela 50 (2008) 1237 (Phys. Solid State 50 (2008) 1287).
[36] I.I. Sobel'man, Introduction to the Theory of Atomic Spectra, Pergamon, Oxford, 1972 (Nauka, Moscow, 1977).
[37] Y. Tanabe, T. Moriya, S. Sugano, Phys. Rev. Lett. 15 (1965) 1023.
[38] A.V. Malakhovskii, G.G. Vasilev, Phys. Stat. Sol. (B) 118 (1983) 337.
[39] B.R. Judd, Phys. Rev. 127 (1962) 750.
[40] G.S. Ofelt, J. Chem. Phys. 37 (1962) 511.
[41] R.D. Peacock, Struct. Bond. 22 (1975) 83–122.
[42] W.F. Krupke, IEEE J. Quant. Electron. QE-7 (1971) 153.
[43] A.A. Kaminskii, L. Li, Phys. Stat. Sol. (A) 26 (1974) K21.
[44] M.J. Weber, T.E. Varitimos, J. Appl. Phys. 42 (1971) 4996.
[45] P. Goldner, F. Auzel, J. Appl. Phys. 79 (1996) 7972.
[46] I.S. Edelman, A.V. Malakhovskii, A.M. Potseluyko, T.V. Zarubina, A.V. Zamkov, J. Non-Cryst. Solids 306 (2002) 120.
[47] W.F. Krupke, IEEE J. Quant. Electron. QE-10 (1974) 450.
[48] V.L. Ginzburg, Theoretical Physics and Astrophysics, Nauka, Moscow, 1975 (Pergamon, Oxford, 1979).
[49] A.A. Kaminskii, L. Li, Phys. Stat. Sol. (A) 26 (1974) 593.
[50] A.A. Kaminskii, Crystalline Lazers: Physical Processes and Operating Schemes, CRS, New York, 1996.
[51] A.S. Aleksandrovsky, A.V. Malakhovskii, A.S. Krylov, V.N. Voronov, J. Luminesc. 132 (2012) 690.